

Electronic Excitation Energy Transfer between Nucleobases of Natural DNA

Ignacio Vayá,^{‡,†} Thomas Gustavsson,[‡] Thierry Douki,[§] Yuri Berlin,^{||} and Dimitra Markovitsi^{*,‡}

[‡]CNRS, IRAMIS, SPAM, Laboratoire Francis Perrin, URA 2453, F-91191 Gif-sur-Yvette, France

[§]CEA, INAC, SCIB, UJF & CNRS, LCIB (UMR_E 3 CEA-UJF and FRE 3200), Laboratoire “Lésions des Acides Nucléiques”, 17 Rue des Martyrs, F-38054 Grenoble Cedex 9, France

^{||}Department of Chemistry, Northwestern University, 2145 Sheridan Road, Evanston, Illinois 60208-3113, United States

S Supporting Information

ABSTRACT: Transfer of the electronic excitation energy in calf thymus DNA is studied by time-resolved fluorescence spectroscopy. The fluorescence anisotropy, after an initial decay starting on the femtosecond time scale, dwindles down to ca. 0.1. The in-plane depolarized fluorescence decays are described by a stretched exponential law. Our observations are consistent with one-dimensional transfer mediated by charge-transfer excited states.

It is well established that absorption of UV radiation by DNA bases induces carcinogenic mutations, triggered by photochemical reactions. The DNA lesions at mutational hotspots are not randomly distributed but depend on the base sequence around them.¹ This dependence could be related to the redistribution of the electronic excitation energy among the bases. Energy transfer was shown to take place in model duplexes on the femtosecond time scale.^{2,3} The ultrafast character of the observed process is due to the delocalized nature of the Franck–Condon excited states, rationalized by theoretical calculations.^{4–6} These studies deal with model duplexes composed of one type of base pairs in a repetitive sequence pattern, favoring a collective behavior. The same behavior has been questioned in the case of natural DNA, where the base sequence is far from regular.⁷ Here we show that energy transfer indeed takes place in genomic calf thymus DNA (CT-DNA) excited at 267 nm. The onset of this process was found to be faster than 150 fs. The transfer proceeds within the nanosecond time domain as may be inferred from the time dependence of the fluorescence anisotropy. This conclusion is also supported by the fit of the fluorescence decays with a stretched exponential function, typical for dispersive rate processes.⁸

CT-DNA (Sigma), composed of 58% adenine-thymine and 42% guanine-cytosine pairs, was purified using a Chelex ion-exchange resin and subsequent extensive dialysis. It was dissolved in phosphate buffer (0.1 M NaH₂PO₄, 0.1 M Na₂HPO₄, and 0.25 M NaCl). Two different detection techniques, fluorescence upconversion (FU) and time-correlated single photon counting (TCSPC), with instrumental response functions of 330 fs and 80 ps, respectively, were used. Fluorescence anisotropy decays $r(t)$ were recorded at 22 °C,

whereas fluorescence decays $I(t)$ were also studied as a function of temperature.

Under excitation at 267 nm, the steady-state fluorescence spectrum of CT-DNA peaks at 327 nm (Figure 1a). This

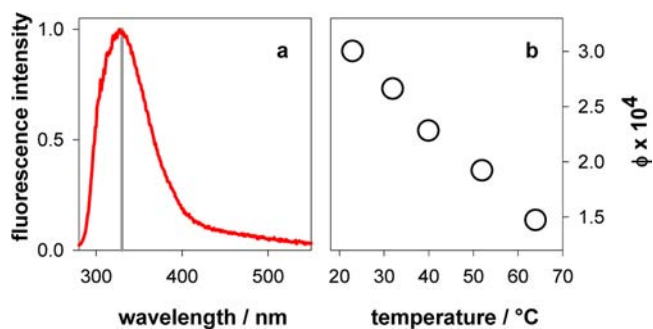


Figure 1. (a) Steady-state fluorescence spectrum of CT-DNA and (b) temperature dependence of the fluorescence quantum yield. Excitation wavelength: 267 nm. The gray line indicates the wavelength at which time-resolved measurements were performed.

spectrum is very similar to that observed for the stoichiometric mixture of mononucleotides.⁹ But in contrast to the monomeric constituents characterized but the fluorescence decay on the sub-picosecond time scale, the CT-DNA fluorescence exhibits multiscale decays ranging from the femtosecond to the nanosecond time domains.⁹ When temperature is below the melting point and increases from 22 to 64 °C, the fluorescence quantum yield decreases by 50% (Figure 1b), whereas the shape of the spectrum remains the same.

The fluorescence anisotropy determined for CT-DNA by FU at 330 nm is presented in Figure 2a, together with the signal obtained for the stoichiometric mixture of mononucleotides.^{2,3} As has been found earlier for model helices, the zero time anisotropy of CT-DNA is lower than that of the monomer mixture. Subsequently, the duplex anisotropy decreases whereas the anisotropy of mononucleotides remains constant. The fluorescence depolarization observed on the femtosecond time scale, when molecular motions are hindered, reveals that CT-DNA exhibits ultrafast energy transfer similarly to the model duplexes. As explained in detail elsewhere,^{2,10} this ultrafast

Received: May 4, 2012

Published: July 5, 2012

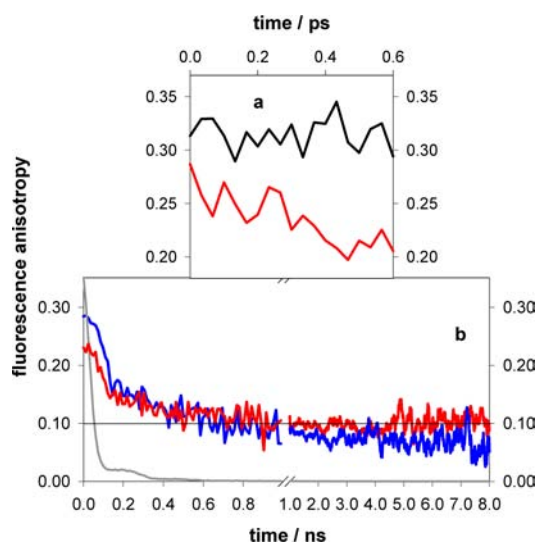


Figure 2. Fluorescence anisotropy decays recorded by FU (a) and TCSPC (b) for CT-DNA in high (phosphate buffer; red) and low (pure water; blue) ionic strength. The black line in (a) corresponds to stoichiometric mixture of a noninteracting mononucleotides. The gray line in (b) represents the instrumental response function.

process results from intraband scattering (internal conversion among exciton states) which is associated to a change in the polarization of the transition vectors.

The fluorescence anisotropy determined for CT-DNA at 330 nm by TCSPC drops down and reaches a constant value of ca. 0.1 in a few hundred picoseconds (Figure 2b). Thereafter, $r(t)$ remains constant over several ns. This time behavior is observed if the ionic strength of the solution is high (phosphate buffer), thus favoring stacking of base pairs. At low ionic strength (ultrapure water), where motions with larger amplitude are possible, $r(t)$ decreases slowly below 0.1 (Figure 2b). Note that in contrast to the long time behavior of the fluorescence anisotropy, the $r(t)$ values at short times are larger for solutions with low ionic strength than for solutions with high ionic strength.

The $r(t)$ value equal to 0.1 is typical for in-plane depolarization of the fluorescence. This implies that the transition dipoles related to photon absorption and emission are randomly distributed perpendicular to an axis.¹¹ In-plane depolarization may result either from physical rotation of a molecule or from the energy transfer in a multichromophoric system. In both cases, the electronic transitions involved remain orthogonal to the rotation axis or the axis of the transfer process, respectively. For linear DNA segments, the $\pi\pi^*$ transitions of the bases are indeed orthogonal to the helix axis. But such segments cannot rotate freely because CT-DNA is a very long macromolecule exhibiting multiple folding. Moreover, fluorescence depolarization due to torsional motions is observed on much longer time scale¹² than the time scale studied in our experiments. In contrast, energy transfer can occur in linear DNA segments, as reported for CT-DNA with intercalated dye molecules.¹³ Our data reveal that the same process takes place when photons are absorbed and emitted directly by DNA.

The dimensionality of the transfer process should be reflected in the associated kinetics. For many one-dimensional disordered systems, the long-time behavior of the kinetics is described by a stretched exponential $\exp[-(t/\tau)^\beta]$, where the

exponent β and the time constant τ depend on the material and fixed external conditions, such as temperature and pressure.¹⁴ Therefore, we fitted the decays of CT-DNA in phosphate buffer recorded as a function of temperature with functions $\exp(-t/\tau_1) + \alpha \exp[-(t/\tau_2)^\beta]$. We assigned to τ_1 a value of 15 ps, which corresponds to our time resolution after deconvolution, and set β equal to 0.5. Note that the exploited fitting function with $\beta = 0.5$ does not support the assumption about the Gaussian diffusion-controlled processes governing the fluorescence decay. In the latter case, one should expect that $I(t) \sim \exp(-\delta t - \gamma t^{0.5})$, with δ and γ being dependent on the diffusion coefficient and the reaction radius (see e.g. ref 15). By using two fitting parameters, α and τ_2 , we obtained reasonable fits; an example is shown in Figure 3a. Upon increasing temperature from 22 to 61 °C, the pre-exponential factor α remains practically constant (0.105 ± 0.005), while τ_2 decreases from 0.55 to 0.32 ns.

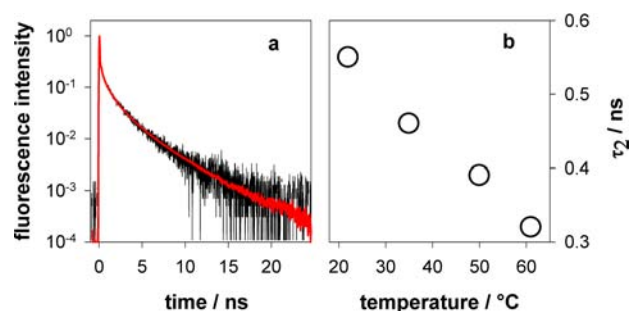


Figure 3. (a) Fluorescence decay of CT-DNA in phosphate buffer at 35 °C (black). In red: fit with the $\exp(-t/\tau_1) + 0.11[\exp-(t/\tau_2)^{0.5}]$ function; $\tau_1 = 15$ ps, $\tau_2 = 0.46$ ns, $\chi^2 = 0.017$. (b) Variation of τ_2 as a function of temperature.

The above-mentioned behavior of the fluorescence anisotropy and fluorescence decays could be attributed to the localized $\pi\pi^*$ excitations performing a random walk along the axis of the double helix. However, two arguments do not support this mechanistic picture. First, according to what is known about model systems, the lifetime of $\pi\pi^*$ states does not exceed a few ps,^{7,16,17} Second, dipolar coupling, which would be driving force for such random walk, allows both intrastrand and interstrand hops, so that the one-dimensional character of the process becomes questionable.⁴

Another plausible explanation is that the random walk process does not take place in the emitting $\pi\pi^*$ state but in a state serving as a reservoir for the bright $\pi\pi^*$. Such dark states could be associated with excited charge-transfer states formed with high yields from the initially populated states, as reported from transient absorption studies on model helices.¹⁶ Theoretical calculations have described various types of excited charge-transfer states, located on the same strand or different strands.⁶ Their energy, very sensitive to environmental factors, may be higher than that of $\pi\pi^*$ states.

The various paths leading to fluorescence of CT-DNA are presented schematically in Figure 4. Photon absorption results in the formation of Frenkel excitons. "Prompt" $\pi\pi^*$ fluorescence arises during the intraband scattering and/or the localization of the excitation. However, this channel makes a minor contribution to the total fluorescence. The main contribution comes from the delayed $\pi\pi^*$ fluorescence resulting from trapping of the excitation by charge-transfer states, followed by charge separation and charge recombination.

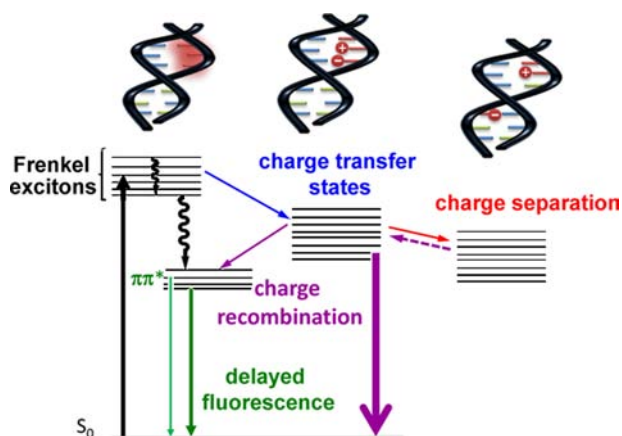


Figure 4. Schematic illustration of the processes underlying fluorescence of CT-DNA. Photon absorption populates excitonic states which may be trapped by excited charge-transfer states; charge separation and charge recombination to $\pi\pi^*$ states gives rise to delayed fluorescence (bold green). Minor contributions to $\pi\pi^*$ fluorescence arise during intraband scattering and/or localization of the excitons (thin green). Charge recombination to the ground state (bold violet) is a major deactivation path.

These processes, which were shown to occur in stilbene-capped DNA hairpins,¹⁸ take place in DNA segments with well stacked bases favoring charge transfer. The channel involving charge separation and charge recombination corresponds to an indirect excitation energy transfer in the sense that different “sites”, and thus different transition dipoles, are involved in photon absorption and emission. These “sites” being randomly distributed around the helix axis, the entire process results to in plane-depolarization of the fluorescence.

Upon increasing conformational motions by decreasing the ionic strength of the solution or by raising the temperature, several of the processes depicted in Figure 4 may be affected. For example, the degree of molecular exciton delocalization diminishes due to increased structural disorder. Moreover, overlap interactions which govern the formation of charge-transfer excited states are reduced because of less efficient base stacking. Consequently, trapping of $\pi\pi^*$ excitations by charge-transfer states becomes less probable and “prompt” emission increases, resulting in higher values of fluorescence anisotropy values at early times (Figure 2b). Finally, charge recombination becomes faster, leading to faster fluorescence decays and lower fluorescence quantum yields.

In summary, we have demonstrated that energy transfer, mediated by dark excited states, takes place in natural DNA. Our study, suggesting interplay between charge and energy transfer, poses new questions, which should inspire further experimental and theoretical work. In particular, it is important to determine the base sequences which may favor charge separation and charge recombination to $\pi\pi^*$ states, the number of sites involved in the transfer process, and its correlation with the formation of UV-induced lesions.

■ ASSOCIATED CONTENT

Ⓢ Supporting Information

Materials and experimental setups. This material is available free of charge via the Internet at <http://pubs.acs.org>.

■ AUTHOR INFORMATION

Corresponding Author

dimitra.markovitsi@cea.fr

Present Address

†Departamento de Química, Universidad Politécnica de Valencia, camino de vera s/n, 46022 Valencia, Spain

Notes

The authors declare no competing financial interest.

■ ACKNOWLEDGMENTS

The French Agency for Research (ANR-10-BLAN-0809-01), the Conselleria de Educacion-Generalitat Valenciana (VALi+D program to I.V., No. 2010033), and ONR/MURI (Y.B.) are acknowledged for financial support.

■ REFERENCES

- (1) Sage, E. *Photochem. Photobiol.* **1993**, *57*, 163–174. You, Y.-H.; Szabo, P. E.; Pfeifer, G. P. *Carcinogenesis* **2000**, *21*, 2113–2117.
- (2) Markovitsi, D.; Onidas, D.; Gustavsson, T.; Talbot, F.; Lazzarotto, E. *J. Am. Chem. Soc.* **2005**, *127*, 17130–17131.
- (3) Miannay, F. A.; Banyasz, A.; Gustavsson, T.; Markovitsi, D. *J. Am. Chem. Soc.* **2007**, *129*, 14574–14575.
- (4) Bouvier, B.; Gustavsson, T.; Markovitsi, D.; Millié, P. *Chem. Phys.* **2002**, *275*, 75–92.
- (5) Bittner, E. R. *J. Chem. Phys.* **2006**, *125*, 094909 (1–12). Burin, A. L.; Armbruster, M. E.; Hariharan, M.; Lewis, F. D. *Proc. Natl. Acad. Sci. U.S.A.* **2009**, *106*, 989–994.
- (6) Starikov, E. B.; Cuniberti, G.; Tanaka, S. *J. Phys. Chem. B* **2009**, *113*, 10428–10435. Lange, A. W.; Herbert, J. M. *J. Am. Chem. Soc.* **2009**, *131*, 3913–3922. Santoro, F.; Barone, V.; Improta, R. *J. Am. Chem. Soc.* **2009**, *131*, 15232–15245.
- (7) Buchvarov, I.; Wang, Q.; Raytchev, M.; Trifonov, A.; Fiebig, T. *Proc. Natl. Acad. Sci. U.S.A.* **2007**, *104*, 4794–4797.
- (8) Berlin, Y. A.; Miller, J. R.; Plonka, A., Eds. Special Issue on Rate Processes with Kinetic Parameters Distributed over Time and Space. *Chem. Phys.* **1996**, *212*. Plonka, A. *Dispersive kinetics*; Kluwer Academic Publishers: Dordrecht, 2001.
- (9) Vayá, I.; Gustavsson, T.; Miannay, F. A.; Douki, T.; Markovitsi, D. *J. Am. Chem. Soc.* **2010**, *132*, 11834–11835.
- (10) Markovitsi, D.; Gustavsson, T.; Talbot, F. *Photochem. Photobiol. Sci.* **2007**, *6*, 717–724.
- (11) Albrecht, A. C. *J. Mol. Spectrosc.* **1961**, *6*, 84–108.
- (12) Millar, D. P.; Robbins, R. J.; Zewail, A. H. *Proc. Natl. Acad. Sci. U.S.A.* **1980**, *77*, 5593–5597.
- (13) Furstenberg, A.; Julliard, M. D.; Deligeorgiev, T. G.; Gadjev, N. I.; Vasilev, A. A.; Vauthey, E. *J. Am. Chem. Soc.* **2006**, *128*, 7661–7669.
- (14) Shlessinger, M. F.; Montroll, A. W. *Proc. Natl. Acad. Sci. U.S.A.* **1984**, *81*, 1280–1283.
- (15) Doi, M. *J. Phys.: A Math. Gen.* **1976**, *9*, 1479–1495.
- (16) Middleton, C. T.; de La Harpe, K.; Su, C.; Law, U. K.; Crespo-Hernández, C. E.; Kohler, B. *Annu. Rev. Phys. Chem.* **2009**, *60*, 217–239.
- (17) Markovitsi, D.; Gustavsson, T.; Vayá, I. *J. Phys. Chem. Lett.* **2010**, *1*, 3271–3276. Schwalb, N. K.; Temps, F. *Science* **2008**, *322*, 243–245. Kwok, W. M.; Ma, C. S.; Phillips, D. L. *J. Phys. Chem. B* **2009**, *113*, 11527–11534.
- (18) Lewis, F. D.; Liu, J. Q.; Zuo, X. B.; Hayes, R. T.; Wasielewski, M. R. *J. Am. Chem. Soc.* **2003**, *125*, 4850–4861. Lewis, F. D.; Zhu, H.; Daublain, P.; Sigmund, K.; Fiebig, T.; Raytchev, M.; Wang, Q.; Shafirovich, V. *Photochem. Photobiol. Sci.* **2008**, *7*, 534–539.